Proceedings of the World Congress on Mechanical, Chemical, and Material Engineering (MCM 2015)
Barcelona, Spain – July 20 - 21, 2015
Paper No. 277

Numerical Modelling of Air Distribution in the Natatorium Supported by the Experiment

Piotr Ciuman, Barbara Lipska, Grzegorz Burda
Silesian University of Technology, Department of Heating, Ventilation and Dust Removal Technology
ul. Konarskiego 20, 44-100 Gliwice, Poland
piotr.ciuman@polsl.pl; barbara.m.lipska@polsl.pl; grzegorz.burda@o2.pl

Abstract **-**The design of air distribution in ventilated natatoriums can be supported by numerical prediction of air, heat, and moisture flow by the CFD method. To make sure that the numerical model predicts correctly the flow phenomena occurring in such objects it is necessary to carry out the experimental validation of calculation results. The aim of presented research was to evaluate the impact of the discretization grid refinement on the numerical calculations of the air parameters distribution in the actual school natatorium. It was performed with the use of CFD software – Ansys CFX, and was supported by the experiment. Three-dimensional numerical model of the object was prepared, for which boundary conditions were obtained on the basis of the measurements in the facility. Numerical results of speed, temperature and specific humidity for the 3 variants of discretization grids, differing in the mesh refinement, were compared. Numerical results of speed, temperature and specific humidity in the occupied zone were validated by comparing with the results of the measurements.

Keywords**:** numerical modelling CFD, discretization grid, experimental validation, natatorium, ventilation, air distribution

1. Introduction

One of the important, yet difficult stages of ventilation design of natatoriums is the selection of air distribution system. It determines to a large extent distribution of air parameters in the facility, especially in the occupied zone. It shapes the thermal comfort, which has an effect on the occupants' evaluation of ventilation work.

Modern ventilation design can be supported in this respect by numerical predictions of air, heat, moisture and gaseous pollutants flow by the CFD method (*Computational Fluid Dynamics*). Numerical calculations make it possible to evaluate thermal comfort conditions and air quality in the natatorium at the design stage of the ventilation.

In the natatorium a series of complex flow phenomena takes place. There occur phenomena connected with the movement of supply air jets, which largely shape the conditions in the room. There are also phenomena connected with the heat transfer, eg. heat gains or losses through the building envelope, heat gains from evaporating water (rough by day, calm by night), sensible heat gains given to the water through convection, heat gains from heaters and lighting. There is also a flow of moisture evaporating from the surface of water and from the surface of the moist floors to the air in the room.

To make sure that the numerical model correctly predicts the phenomena and can be used in practice, it is necessary to experimentally identify characteristics of such facilities. It's crucial for the appropriate selection of boundary conditions for calculations and for the validation of calculation results with the use of the measurements' values or air parameters obtained in the real facility.

The issue of numerical modelling CFD of airflow in natatoriums was discussed by Li and Heiselberg (2005), Lipska et al. (2010), and also Abo Elazm and Shahata (2015), who numerically and experimentally examined the impact of supply jets on the moisture emission from the pool.

The aim of presented research was to evaluate the impact of discretization grid refinement on numerical calculations results of the air parameters distributions in the actual school natatorium, with the use of CFD software, Ansys CFX, and supported experimentally.

2. Description of The Natatorium and its Numerical Model

The facility used for tests was the actual school natatorium in Gliwice (Poland) (Fig. 1.), with dimensions: length 17,55 m, width 11,6 m and the average height 4,35 m. The dimensions of the pool were: length 12,5 m, width 7 m.

Internal partitions of the tested natatorium were: the north-east wall and the south-east wall and the floor of the natatorium. The rest of the partitions were external. In the south-west wall were windows. Around the pool was a region called the beach.

The natatorium was ventilated by the supply-exhaust ventilation. The air was supplied into the natatorium by 7 inlet grilles mounted in the supply duct in the suspended ceiling along the north part of the beach and by the 12 inlet slots located at the bottom along the windows. The air was exhausted by the 12 outlet grilles mounted in the exhaust duct in the ceiling recess (6 outlet grilles on opposite sides of the recess).

The numerical model of the tested natatorium, presented in fig. 2, was prepared with the use of CFD software – Ansys CFX. Actual dimensions of the natatorium, its geometry and water surface were taken into consideration and the distribution system of ventilation air was modelled.

The inlet grilles were modelled as rectangles with dimensions: 0,31 m x 0,11 m; inlet slots as rectangles with width 0,002 m and average length 0,87 m; similarly, the outlet grilles, with dimensions 0,31 m x 0,11 m. Radiators and lamps were modeled as well.

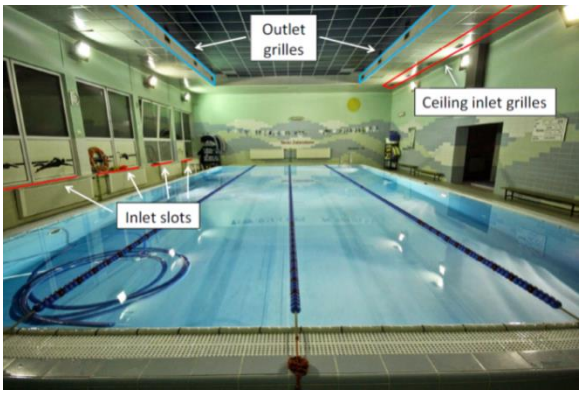

Fig. 1. The view of the interior of the tested school natatorium (Web-1)

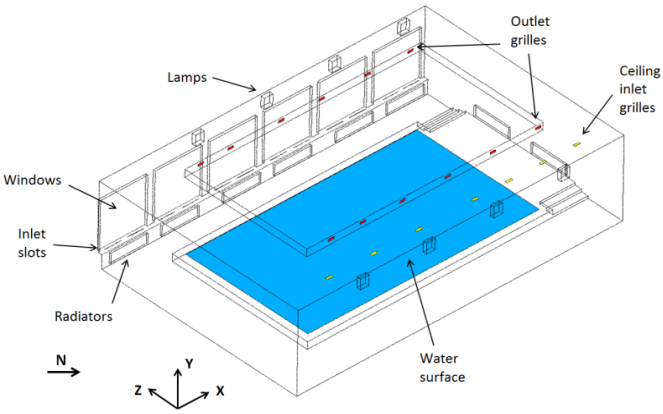

Fig. 2. The numerical model of the natatorium

3. Preparation of the Boundary Conditions

The boundary conditions for numerical calculations were prepared on the basis of the facility stocktaking and results of the air parameters measurements carried out in the natatorium.

These measurements included: measurement of speed and temperature of supply air in inlets with the use of Testo-435 thermo-anemometer, measurement of relative humidity of supply air in inlets with the use of the AR235 APAR temperature and relative humidity register and measurement of pool water temperature with the use of DRT-10 Sensor thermometer. Temperature and relative humidity of the outside air was read on the basis of the data provided by the local meteorological station, located at a distance of 635 m from the natatorium. These parameters could be used as a basis to determine the value of specific humidity, due to the fact that in the air ventilation unit neither dehumidifying nor humidifying of ventilation air occurred. Heat transfer coefficients of building partitions were adopted on the basis of stocktaking of the facility.

Based on the measurements, the boundary conditions were calculated: mass flow of air supplied through ceiling inlet grilles and inlet slots, water surface temperature, mass flow of evaporating moisture from the water surface and moist floors. Convective and radiation heat flows, from radiators and lamps were determined on the basis of known values of their power.

The boundary conditions for the natatorium are presented in table 1.

Table. 1. The boundary conditions for the natatorium

<table>
<tr><td rowspan="4">Mass flow of supply air</td><td colspan="2">Ceiling inlet grilles</td></tr>
<tr><td colspan="2">0,025 kg/s</td></tr>
<tr><td colspan="2">Inlet slots</td></tr>
<tr><td colspan="2">0,020 kg/s</td></tr>
<tr><td>Supply air temperature</td><td colspan="2">36^{o}C</td></tr>
<tr><td>Outside air temperature</td><td colspan="2">9^{o}C</td></tr>
<tr><td>Specific humidity of supply air</td><td colspan="2">0,00409 kg H_2O/kg of dry air</td></tr>
<tr><td>Water temperature</td><td colspan="2">31^{o}C</td></tr>
<tr><td>Water surface temperature</td><td colspan="2">29,75^{o}C</td></tr>
<tr><td>Mass flow of evaporating moisture from the water surface</td><td colspan="2">0,0023 kg/s</td></tr>
<tr><td>Mass flow of evaporating moisture from the moist floors</td><td colspan="2">0,00105 kg/s</td></tr>
<tr><td rowspan="2">Heat flow from a single lamp</td><td>Radiation</td><td>Convection</td></tr>
<tr><td>395,2 W/m^2</td><td>592,8 W/m^2</td></tr>
<tr><td rowspan="2">Heat flow from a single radiator</td><td>Radiation</td><td>Convection</td></tr>
<tr><td>462,8 W/m^2</td><td>694,2 W/m^2</td></tr>
</table>

4. Selection of Discretization Grids and Calculation Procedure

Numerical calculations were carried out with the use of Ansys CFX software, in steady, non-isothermal conditions. In simulations SST turbulence model from EVM models group was used, as well as standard prandtl wall functions.

In numerical simulations 3 variants of unstructured discretization grids were used, built mainly with tetrahedral elements. They are presented in a form of cross-sections in fig. 3. In the grid 1 default settings of the Ansys's mesh generator were used. The grid 2 represented a compromise between the accuracy of calculations and time expenditure required for calculations with the available server. In the grid 2 the additional refinement of mesh elements above the water surface was introduced. Characteristic parameters of these grids are listed in table 2.

Table. 2. The parameters of tested discretization grids

Grid	Constant edge length, *m*	Radius of the refinement influence, *m*	Refinement cell edge length at the surface of inlets and outlets, *m*	Total number of elements	Total number of nodes
1	0,55	-	-	98 756	26 566
2	0,1	-	0,01	8 939 016	1 797 740
3	0,1	0,05 (0,2 m above the water surface)	0,01	10 105 448	2 015 095

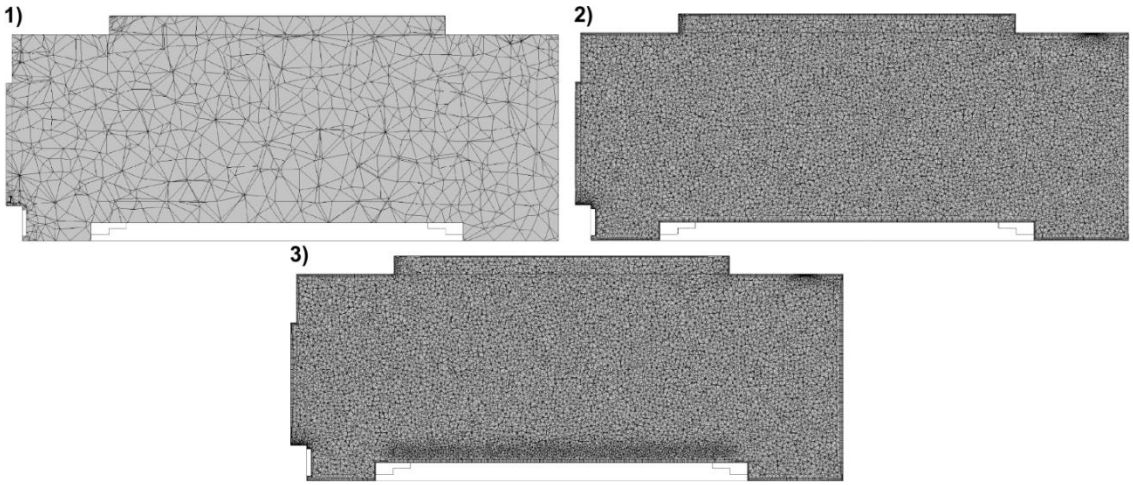

Fig. 3. The tested variants of discretization grids in the plane X = 4,2 m

5. Results of Numerical Calculations

Results of numerical calculations were presented in the form of parameters' maps for each discretization grid in two planes: X = 4,2 m (passing through the ceiling inlet grill and the inlet slot) and Y = 0,6 m (0,2 m above the water surface). Distributions of speed, temperature and specific humidity were analyzed.

In fig. 4. the maps of air averaged speed in the natatorium are shown. From the observation of distribution of this parameter in the vertical section (a), it was concluded that the air jet flowing from the inlet slot washed the window and then changed its flow direction and stuck to the ceiling. This kind of a jet flow, justified physically, was better represented with the use of grids 2 and 3, for which the maps were similar. Also, it is possible to notice the different range of the jet supplied by the ceiling inlet grill for the variant 1 (shorter jet) in comparison with variants 2 and 3 (longer jet). On the maps in the horizontal section in occupied zone (b) a similar distribution of averaged speed was noticed with the use of each discretization grid. This distribution wasn't uniform and speed values varied within the range of 0,012 m/s to 0,5 m/s (locally). The average value was 0,08 m/s. The highest values were observed above the water with the use of grids 2 and 3. It wasn't possible to capture this region using the grid 1. Introducing in the variant 3 the grid refinement above the water surface didn't contribute to predicting different speed values than in the variant 2.

In fig. 5. distribution of air temperature in the natatorium is presented. On the maps in the vertical section it is possible to notice that the distribution of air temperature in the natatorium was largely aligned. However, the values obtained with the use of the grid 1 were higher on average by 1 K in comparison with the results from the other variants. Above the water, in each of the variants, was the layer of a temperature lower by 1 K compared to the rest of the facility. On the maps in the horizontal section in the occupied zone distribution of temperature predicted in the variant 1 was different than in case of other variants. In the variant 1 the region of a higher temperature near the windows was clearly visible; it didn't appear in other variants. All along the beach predicted temperature value was higher by 1 K compared to variants 2 and 3, in which the rise of the temperature occurred only locally. However generally, predicted distributions differed among themselves only minimally.

In fig. 6. distribution of air specific humidity in the natatorium is presented. The differences between the values obtained with the use of each of the discretization grids are clearly visible. On the maps in the vertical section in each variant a region of higher values of specific humidity above the water surface and floor was predicted. The distributions received with the use of grids 1 and 2 were similar. In the higher part of the facility the value of specific humidity decreased and it increased again near the ceiling. The distribution obtained for the grid 3 differed significantly. The region of higher specific humidity occurred only above the water surface and in the rest of the natatorium the values were much lower. On the maps in the horizontal section diversity in the size of the region of the highest values of specific humidity

between the variants was observed. For the variant 1 the specific humidity value in the most part of the natatorium was higher than in the variant 2, in which higher values occurred mainly above the water surface. With the use of the grid 3 lower values were predicted with local maxima above the water surface.

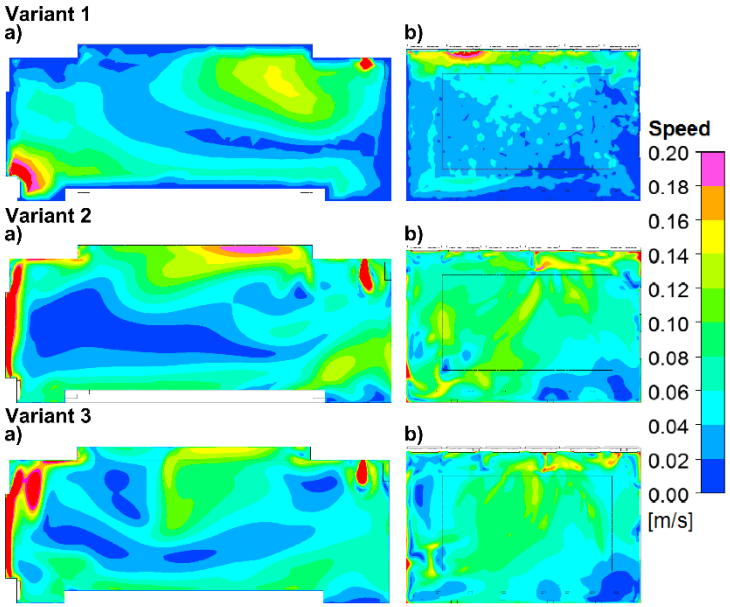

Fig. 4. Distribution of air averaged speed in the natatorium for three variants of discretization grids in the plane: a) X = 4,2 m, b) Y = 0,6 m (0,2 m above the water surface)

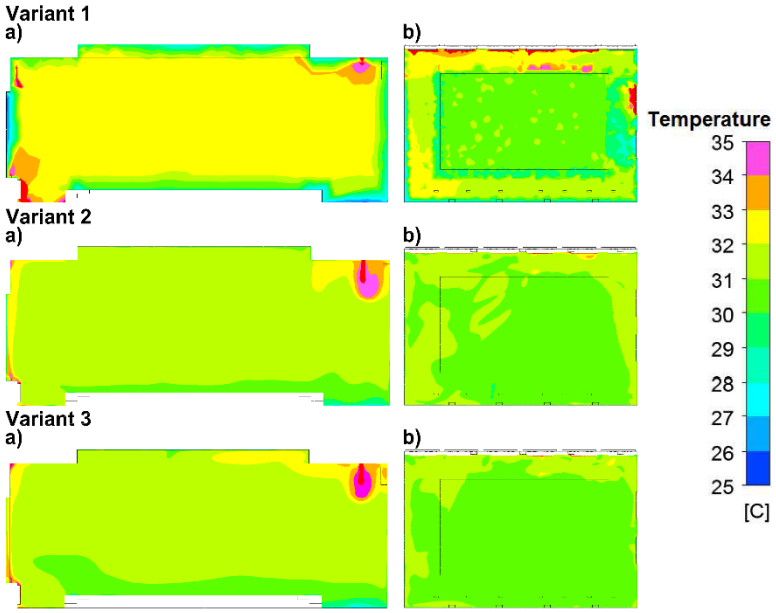

Fig. 5. Distribution of air temperature in the natatorium for three variants of discretization grids in the plane: a) X = 4,2 m, b) Y = 0,6 m (0,2 m above the water surface)

6. The Validation of Calculation Results

The validation was performed for the predicted values of averaged speed, temperature and specific humidity obtained with the use of tested discretization grids by comparison with the measurement values obtained in the real facility. The measurements were carried out with the use of the SENSOANEMO

5100SF Sensor thermos-anemometers with the omnidirectional, spherical speed sensors and the AR235 APAR temperature and relative humidity registers. The measurements took place in 6 measuring axes P1 - P6, deployed evenly in the middle of the beach width on four levels - 0,1 m; 0,6 m; 1,1m; 1,7 m and in two points above the water surface (W1 and W2) at the height of 0,6 m (0,2 m above the water surface).

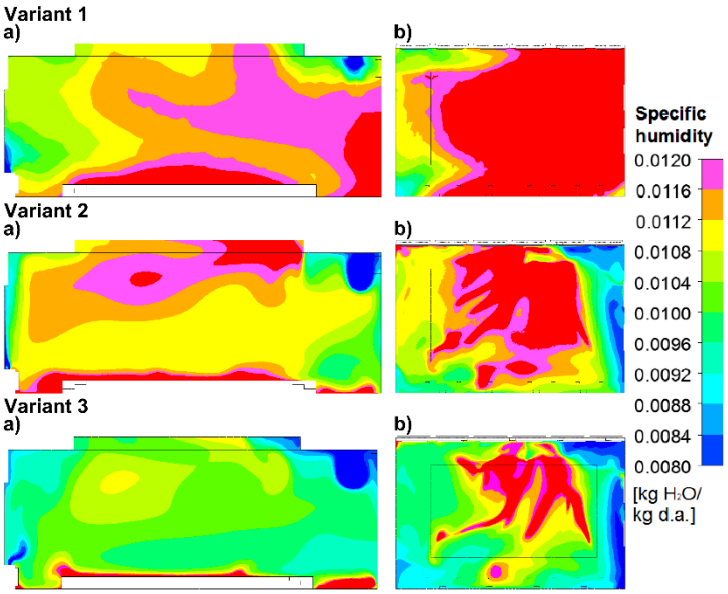

Fig. 6. Distribution of air specific humidity in the natatorium for three variants of discretization grids in the plane: a) X = 4,2 m, b) Y = 0,6 m (0,2 m above the water surface)

In fig. 7 - 9 the examples of these parameters validation results are presented for the measuring axis P2, located on the side of the windows, and for the measuring point W1, located on the side of the inner wall. The most close to the measured values results of calculated averaged speed in the axis P2 were predicted by the variant 1 of the grid, although differences between the results for each variant were minimal (fig. 7.). On the higher levels of the measuring axis the values were in the range of thermo-anemometer's measuring error. The biggest departure from the measuring value occurred at the height of 0,1 m. In the point W1 the results for variant 2 and 3 were identical with the measurement. The results for the variant 1 were within the range of measuring error.

It should be noted that predicted and measured values of averaged speed deviated from the values recommended by Kappler (1977): 0,15 - 0,20 m/s. It resulted in the stillness of the air in the occupied zone, which was felt during the measurements.

The predicted temperature values in the axis P2 were higher on average by 4 K than the measurement values (fig. 8.). The most similar results were obtained using the grid from the variant 3. The situation looked similar in case of the point W1. The best results were obtained also for the grid 3, but still differed by about 3 K from the measurement. According to the VDI 2089 Standards air temperature should be about 2 ÷ 4^{o}C higher than water temperature. In the tested natatorium water temperature was 31^{o}C, therefore the air temperature should be 33 ÷ 35^{o}C. However, the measured values didn't fit this range.

As for the specific humidity values in the axis P2, the most similar results to those measured were obtained with the use of the grid from variant 3 (fig. 9.), with the exception of the point at 0,1 m. The values were within the range of measuring error of the instrument or deviated from it slightly. It looked similar in case of the point W1, for which the most similar calculation result to the measurement was obtained for the grid 3. In accordance with the VDI 2089 Standards the air specific humidity in the natatorium should be within the range 40 ÷ 64^{o}C, which means, in terms of recommended temperature values, that specific humidity should be 0,0135 ÷ 0,023 kg H_2O/kg d.a. The measured values in the

natatorium were similar to the lower end of this range, but only the value at the height of 1,7 m was actually within the range.

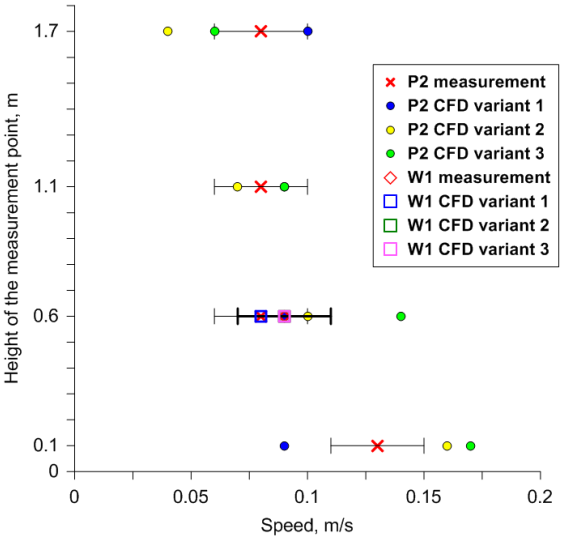

Fig. 7. The validation of averaged speed value for three variants of discretization grids for the measurement axis P2 and W1 point

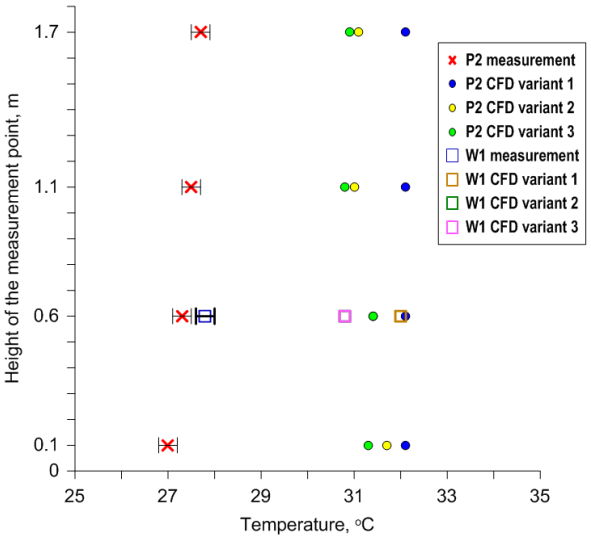

Fig. 8. The validation of temperature value for three variants of discretization grids for the measurement point P2 and W1 point

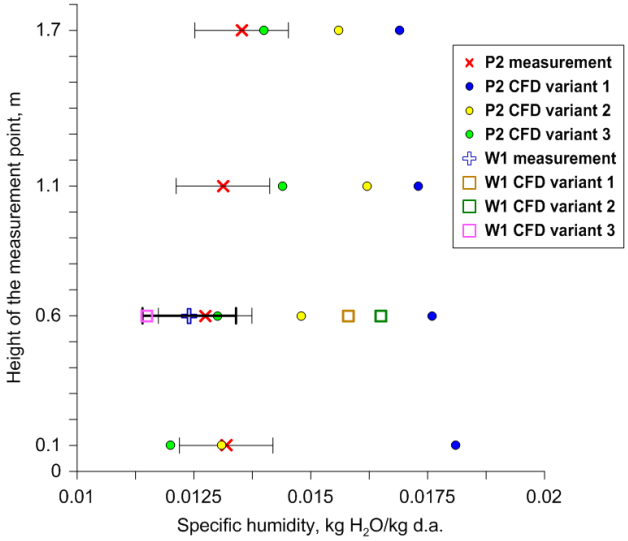

Fig. 9. The validation of specific humidity value for three variants of discretization grids for the measurement point P2 and W1 point

7. Conclusion

1. With The Use Of Numerical Modelling Cfd It Was Possible To Reproduce The Basic Phenomena Of Air, Heat And Moisture Flow Occurring In The Ventilated Natatorium.
2. The Refinement Of Discretization Grid Had An Influence On Predicted Distributions Of Air Speed And Temperature In The Natatorium. For The Tested Discretization Grids The Range Of Analyzed Parameters Values Was Similar. However, Introducing The Refinement Caused The Change Of Their Distributions In Vertical And Horizontal Sections In The Occupied Zone. The Additional Grid Refinement Above The Water Surface Caused The Change Of Distributions In This Region.

3. The Refinement Of Discretization Grid Affected The Range Of Air Specific Humidity Values. The Additional Refinement Above The Water Surface Was Especially Important, As It Strongly Affected The Range Of Values And Their Distribution, Not Only In This Region But In The Whole Facility.
4. The Validation Of Averaged Speed Values For The Measurement Axis P2 Showed That, Regardless Of The Discretization Grid, The Predicted Values Deviated Slightly From The Measured Values And Were Mostly Within The Range Of The Thermo-Anemometers' Measuring Error. The Grid Refinement Above The Water Surface Improved The Accuracy Of Averaged Speed Calculations At The Point W1.
5. The Validation Of The Temperature Value Showed That Prediction Of The Values Close To The Measurement Results Wasn't Possible. They Were Higher By About 3 ÷ 4 K From The Measured Ones. This Could Be Due To The Inaccuracy In Reproducing Heat Loses Trough The Building Envelopes. The Analysis Of Causes And Their Elimination Will Be The Subject Of Further Research.
6. The Refinement Of Discretization Grid, Especially Above The Water, Highly Increased The Accuracy Of Predicting Specific Humidity. Its Predicted Values Were Within The Range Of Measuring Error Or Slightly Deviated From It.

References

Abo Elazm, M. M., & Shahata, A. I. (2015). Numerical and Field Study of the Effect of Air Velocity and Evaporation Rate on Indoor Air Quality in Enclosed Swimming Pools. *International Review of Mechanical Engineering (IREME),* 9(1), 97-103.

Kappler, H. P. (1977). Baseny Kąpielowe. *Arkady*, Warszawa 1962.

Koper, P., Lipska, B., & Michnol, W. (2010). Assessment Of Thermal Comfort In Indoor Swimming Pool Making Use Of The Numerical Prediction CFD. *ACEE,* 3, 95-104.

Li, Z., & Heiselberg, P.K. (2005). CFD Simulations for Water Evaporation and Airflow Movement in Swimming Baths. *Instituttet for Bygningsteknik*, Aalborg Universitet.

VDI 2089 Blatt 1 Technische Gebäudeausrüstung von Schwimmbädern – Hallenbäder.

Web sites:

Web-1: http://tinyurl.com/pm5hyau, consulted 24 Apr. 2015.